JCTC Journal of Chemical Theory and Computation

pubs.acs.org/JCTC Article

Ground- and Excited-State Dipole Moments and Oscillator Strengths of Full Configuration Interaction Quality

Yann Damour,* Raúl Quintero-Monsebaiz, Michel Caffarel, Denis Jacquemin, Fábris Kossoski, Anthony Scemama, and Pierre-François Loos*

Cite This: *J. Chem. Theory Comput.* 2023, 19, 221−234 Read Online

ACCESS | Metrics & More | Article Recommendations | Supporting Information

ABSTRACT: We report ground- and excited-state dipole moments and oscillator strengths (computed in different "gauges" or representations) of full configuration interaction (FCI) quality using the selected configuration interaction method known as *Configuration Interaction using a Perturbative Selection made Iteratively* (CIPSI). Thanks to a set encompassing 35 ground- and excited-state properties computed in 11 small molecules, the present near-FCI estimates allow us to assess the accuracy of high-order coupled-cluster (CC) calculations including up to quadruple excitations. In particular, we show that incrementing the excitation degree of the CC expansion (from CC with singles and doubles (CCSD) to CC with singles, doubles, and triples (CCSDT) or from CCSDT to CC with singles, doubles, triples, and quadruples (CCSDTQ)) reduces the average error with respect to the near-FCI reference values by approximately 1 order of magnitude.

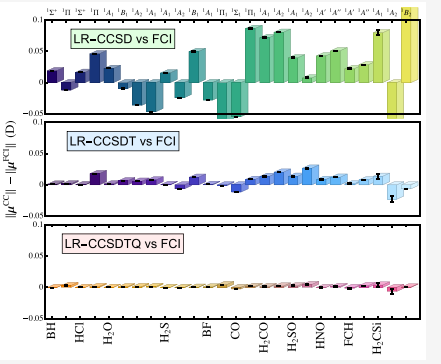

I. INTRODUCTION

The study of electric dipole moments and oscillator strengths is a major endeavor in electronic structure theory. The electric dipole moment is a vector that characterizes the intensity and the orientation of an electric dipole, and its direction and magnitude are dictated by the distribution of the electric charges. In a chemical system, it corresponds to the charge distribution of the electrons and nuclei and is consequently related to its electronic structure.

From an experimental point of view, the dipole moment is a physical "signature" of a system in a given electronic state. Thus, it can be used to characterize unknown species or a specific isomer.[1−3] In addition, the electric dipole moment is central in spectroscopy. For example, vibrational modes are said to be infrared-active if they are accompanied by a change in the electric dipole moment.[4]

From a more theoretical point of view, combining dipole moment and potential energy surfaces allows us to model energies and intensities of vibrational−rotational transitions and is then useful for rovibrational spectroscopy.[5−7] Furthermore, because the dipole moment is intimately linked to the charge distribution of the system in a given state, it is closely related to its electronic density and wave function. Consequently, dipole moments are often considered descriptors of the quality of the electronic density for both ground and excited states.[8,9]

Another interesting physical quantity also classified as dipolar is the oscillator strength.[10] Because the oscillator strength is linked to the transition probability between two states (i.e., the transition dipole moment), it tells us whether or not a transition is (electric-)dipole-allowed. Indeed, the magnitude of the oscillator strength is directly connected to the intensity of the peaks in ultraviolet−visible spectra.

One of the main goals in theoretical quantum chemistry is to describe accurately the electronic structure of chemical systems by solving the Schrödinger equation, which gives access to experimentally measurable properties such as dipole moments and oscillator strengths. Unfortunately, an accurate description of the electronic structure requires one to approach satisfactorily the solution of the Schrödinger equation through an appropriate and judicious set of approximations.[11−13]

The mean-field Hartree−Fock (HF) approximation[11] is a relatively cheap method and is the starting point of correlated treatments in wave function methods. HF is known to produce reasonably accurate properties but breaks down when correlation effects become predominant. One textbook example is the ground-state dipole moment of CO which is predicted with the wrong orientation at the HF level.[11,14] This disagreement disappears when one takes into account correlation effects. On the opposite side, the full configuration interaction (FCI) method provides the exact solution of the Schrödinger equation within a given one-electron basis set by constructing the wave function as a linear combination of all

Received: November 8, 2022
Published: December 22, 2022

possible electronic configurations.[15−19] All these configurations, which can be represented as Slater determinants, form the so-called Hilbert space that, unfortunately, grows exponentially fast with the system size, leading to a prohibitive computational cost for real-life molecules. Thankfully, between these two extremes, HF and FCI, a plethora of methods, some with systematic improvability, have been developed.

To reach FCI from HF, the most natural route is likely to increase systematically the maximum excitation degree of the configuration interaction (CI) wave function with respect to a reference configuration (usually taken as the HF ground-state determinant). This leads to excitation-based CI which has polynomial scaling but lacks size extensivity/consistency. By taking into account all single and double excitations, one gets CI with singles and doubles (CISD) with a computational cost scaling as $O(N^6)$ (where N is the number of one-electron basis functions), while adding the triples yields CI with singles, doubles, and triples (CISDT) scaling as $O(N^8)$, and so on. Alternatively, one can systematically increase the seniority number (i.e., the number of unpaired electrons) or the hierarchy parameter (average of the excitation degree and half the seniority number).[20−22] Unfortunately, all these methods require considering a huge number of electronic configurations, most of them contributing very little to the energies and/or properties of interest.

This suggests the need for a selection of determinants based on an adequate predetermined criterion to capture effectively the electronic configurations contributing the most to a given quantity. The use of such criteria to build CI wave functions is the central idea of a general class of iterative methods known as selected CI (SCI), which sparsely explores the Hilbert space by selecting only the "most important" determinants for a target property.[23−28] In most of them, this iterative selection process is performed via an energetic perturbative criterion, and determinants with the largest contributions are added to the variational space.[23−25,29−38] A second-order perturbative correction (PT2) is usually computed on top of this variational treatment.[30,31,34,37,39−41] The resulting SCI+PT2 methods provide a much faster energy convergence with the size of the wave function than standard CI approaches.[30,35,39,42−51] Importantly, as a post-treatment, the SCI+PT2 energy and properties are usually extrapolated to the FCI limit using various strategies.[42,46,52]

Relying on an exponential *ansatz* of the wave function, coupled cluster (CC) methods provide an alternative, size-extensive, and systematically improvable route (with polynomial scaling) to the FCI limit.[53−58] Following a similar philosophy as excitation-based CI, by adding successively higher excitation levels, one gets CC with singles and doubles (CCSD);[59−63] CC with singles, doubles, and triples (CCSDT);[64−67] CC with singles, doubles, triples, and quadruples (CCSDTQ),[68−72] with respective computational cost scaling as $O(N^6)$, $O(N^8)$, and $O(N^{10})$. Furthermore, each of these methods can be made cheaper without altering too much their accuracy via the CC*n* family of methods: CC2 (N^5),[73,74] CC3 (N^7),[75−79] and CC4 (N^9).[80−83]

Excited-state energies and properties can be straightforwardly obtained within the CI formalism by looking for higher roots of the CI matrix and their corresponding eigenvectors. Likewise, one can access excited states at the CC level in the equation-of-motion (EOM)[62,66,84−88] or linear-response (LR)[61,86,89−91] frameworks. Although they yield identical excitation energies, the excited-state properties produced by these two formalisms differ and are equal only when the FCI limit is reached.[57] For the same excitation degree (hence the same computational scaling), the (nonvariational) CC methods are generally more accurate than their (variational) CI counterparts for the computation of ground- and excited-state energies and properties, especially in the Franck−Condon region.[71,72,80] This explains why high-order CC methods have now become the workhorse of electronic structure theory when one is looking for high accuracy. Nonetheless, their overall accuracy (with respect to FCI) remains very hard to assess, especially in the case of properties that are usually more sensitive than excitation energies to the level of theory and the one-electron basis set.[9,92−95]

Another feature that makes the calculation of electric (and magnetic) properties challenging is that there exist two different pathways for computing them which only become equivalent in the FCI limit but differ for approximate methods where the wave function is not fully variational with respect to all parameters.[13,96,97] The first and most natural way consists in calculating the properties as expectation values of the corresponding operator associated with the physical observable of interest. The second approach, based on the Hellmann−Feynman theorem, requires the derivative of the energy with respect to a given external perturbation linked to the observable.[96,98,99] Importantly, none of these formalisms can claim to be superior in general, although, in some cases, it has been observed that the derivative approach is likely more accurate.[100] The energy derivative technique has been first developed by Pulay in the context of self-consistent field methods,[98] followed by others in many-body perturbation theory,[96,101−104] CI,[105−113] and CC methods.[71,114−120] Recently, several groups have reported the implementation of nuclear gradients (i.e., energy derivatives with respect to the nuclear displacements) for SCI-SCF[121−123] and related[124] methods.

The expectation value route is usually more straightforward in terms of implementation, but one must have access explicitly to the wave function and/or to the corresponding reduced density matrices, which is not always possible. For approximate wave functions, it has been observed that the derivative formalism is likely to lead to more accurate properties because additional contributions are taken into account.[125,126] In this context, the Lagrangian formalism, developed by Helgaker and co-workers,[97,127−129] provides a rigorous mathematical framework to take into account the variation of the wave function parameters. For example, taking or not into account the response of the orbital coefficients to the external perturbation leads to the so-called "orbital-relaxed" and "orbital-unrelaxed" properties.[130] The Lagrangian formalism is employed extensively in LR-CC where the relaxation of the ground-state CC amplitudes is considered, in contrast to the cheaper EOM-CC method, resulting in size-intensive transition properties.[131]

Unfortunately, orbital relaxation effects may cause small discrepancies when employed within the frozen-core approximation since the orbital response depends on all the orbitals, even those that are frozen.[132] Therefore, within the frozen core approximation, the orbital-relaxed and orbital-unrelaxed dipole moments can slightly differ even at the FCI level. This is typically the case when one considers small molecules with a significant number of frozen orbitals compared to the number of active ones.

https://doi.org/10.1021/acs.jctc.2c01111
J. Chem. Theory Comput. 2023, 19, 221−234

Another degree of flexibility in the calculation of properties concerns the "gauges" or, more correctly, representations[133] (length, velocity, or mixed) chosen to compute quantities like the oscillator strength, which are equal only for the exact wave function, i.e., at the FCI limit and in a complete basis set[92,134] (or in the complete basis set limit for approximate methods[135] which fulfill the Thomas−Reiche−Kuhn sum rule[136−138]). Accordingly, gauge invariance can be employed to evaluate the degree of completeness of the one-electron basis set.[139]

The present work reports ground- and excited-state dipole moments as well as oscillator strengths (computed in different representations) of FCI quality obtained with the SCI method known as *Configuration Interaction using a Perturbative Selection made Iteratively* (CIPSI)[24] for a set of 11 small molecules extracted from the recent work of Chrayteh et al.[140] Thanks to the high accuracy of the present results, we can systematically assess the overall accuracy of high-order CC methods for these properties and validate the quality of the theoretical best estimates (TBEs) reported in ref 140.

At this stage, it is worth mentioning that works on dipole moments at the SCI level have been previously reported in the literature. For example, the seminal work of Angeli and Cimiraglia reports a tailored selection procedure for dipole moments via a modification of the CIPSI algorithm.[27] Although restricted to small wave functions, these authors achieved a significant speed-up of the convergence of the latter property and generalized it to other one-electron properties. On the other hand, Giner et al. studied the effect of self-consistency in the context of density-based basis-set corrections[94,141−143] on ground-state dipole moments using very accurate CIPSI calculations.[9] Another study worth mentioning is the work of Eriksen and Gauss[144] who reported (transition) dipole moments of LiH and MgO in large augmented basis sets using the many-body expanded FCI method[145−148] which provides an interesting alternative to SCI methods.[52] Other relevant studies have been performed using Monte Carlo CI[149] or FCI quantum Monte Carlo.[150]

Additionally, benchmark studies of wave function and density-based methods have been reported for both dipole moments and oscillator strengths. For example, Hait et al. produced 200 benchmark values of ground-state dipole moments using CCSD(T) and basis set extrapolation to assess 88 popular or recently developed exchange−correlation functionals.[151] More recently, Chrayteh et al.[140] reported very accurate ground- and excited-state dipole moments, in addition to oscillator strengths, using LR-CC up to quintuples and applying basis set extrapolation for a set of small molecules. In a follow-up paper, using these reference data, Sarkar et al. reported an extensive benchmark study of several single-reference wave function methods and time-dependent density-functional theory for several exchange−correlation functionals.[93] The impact of the representations, the formalism (LR vs EOM), and the effect of orbital relaxation (relaxed vs unrelaxed) were carefully analyzed. Although these three works focused on very accurate values for small molecules, one can also find a large panel of benchmark studies devoted to larger compounds for which it is obviously harder to establish indisputable reference values.[130,152−170]

The present paper is organized as follows. Section II recalls the working equations of the CIPSI algorithm and how one computes dipole moments and oscillator strengths at the SCI level. Section III reports our computational details, while in Section IV, we discuss the present results and explain in detail how we reach the FCI limit via tailored extrapolation procedures. Our conclusions are drawn in Section V. Unless otherwise stated, atomic units are used throughout.

II. THEORY

II.A. Selected Configuration Interaction. As mentioned above, SCI methods are part of the family of truncated CI methods. Usually, their energy is defined as the sum of a variational part and a second-order perturbative contribution. The definition of each contribution is provided below.

The (zeroth-order) variational wave function associated with the kth state ($k = 0$ being the ground state) is

$$|\Psi_k^{\mathrm{var}}\rangle = \sum_{I\in\mathcal{I}} c_{Ik}|I\rangle \tag{1}$$

where $|I\rangle$ are determinants belonging to the internal (or model) space $\mathcal{I}$. Assuming that it is normalized, this wave function has the variational energy

$$E_k^{\mathrm{var}} = \langle\Psi_k^{\mathrm{var}}|\hat{H}|\Psi_k^{\mathrm{var}}\rangle \tag{2}$$

where $\hat{H}$ is the usual (nonrelativistic) molecular Hamiltonian

$$\hat{H} = -\sum_i \frac{\nabla_i^2}{2} - \sum_i\sum_A \frac{Z_A}{|\boldsymbol{r}_i - \boldsymbol{R}_A|} + \sum_{i<j}\frac{1}{|\boldsymbol{r}_i - \boldsymbol{r}_j|} + \sum_{A<B}\frac{Z_A Z_B}{|\boldsymbol{R}_A - \boldsymbol{R}_B|} \tag{3}$$

and $\boldsymbol{r}_i$ is the coordinate of the ith electron while Z_A and $\boldsymbol{R}_A$ are the charge and position of the Ath nucleus, respectively. The associated (first-order) perturbative wave function is

$$|\Psi_k^{\mathrm{pert}}\rangle = \sum_{\alpha\in\mathcal{A}} c_{\alpha k}|\alpha\rangle \tag{4}$$

where the determinants $|\alpha\rangle$, known as perturbers, belong to the external (or outer) space $\mathcal{A}$.

Employing the Epstein−Nesbet partitioning, i.e.

$$\hat{H}^{(0)} = \sum_{IJ}|I\rangle H_{IJ}\langle J| + \sum_\alpha |\alpha\rangle H_{\alpha\alpha}\langle\alpha| \tag{5a}$$

$$\hat{H}^{(1)} = \hat{H} - \hat{H}^{(0)} \tag{5b}$$

with $H_{IJ} = \langle I|\hat{H}|J\rangle$ and $H_{\alpha\alpha} = \langle\alpha|\hat{H}|\alpha\rangle$, we have $\langle\Psi_k^{\mathrm{var}}|\hat{H}^{(1)}|\Psi_k^{\mathrm{var}}\rangle = 0$ and

$$E_k^{\mathrm{PT2}} = \langle\Psi_k^{\mathrm{pert}}|\hat{H}^{(1)}|\Psi_k^{\mathrm{var}}\rangle \tag{6}$$

where the second-order perturbative energy can be conveniently recast as

$$E_k^{\mathrm{PT2}} = \sum_\alpha e_{\alpha k}^{\mathrm{PT2}} = \sum_\alpha \frac{\langle\alpha|\hat{H}|\Psi_k^{\mathrm{var}}\rangle^2}{E_k^{\mathrm{var}} - H_{\alpha\alpha}} \tag{7}$$

The SCI+PT2 energy of the kth excited state is thus given by the sum $E_k^{\mathrm{var}} + E_k^{\mathrm{PT2}}$. The iterative procedure of the CIPSI algorithm is schematically represented in Figure 1 in the case of a single-state calculation. We refer the interested reader to ref 37 for additional details.

II.B. Properties as Expectation Values. Here we follow the approach based on the expectation value of the corresponding operator to compute properties at the SCI level.

https://doi.org/10.1021/acs.jctc.2c01111
J. Chem. Theory Comput. 2023, 19, 221−234

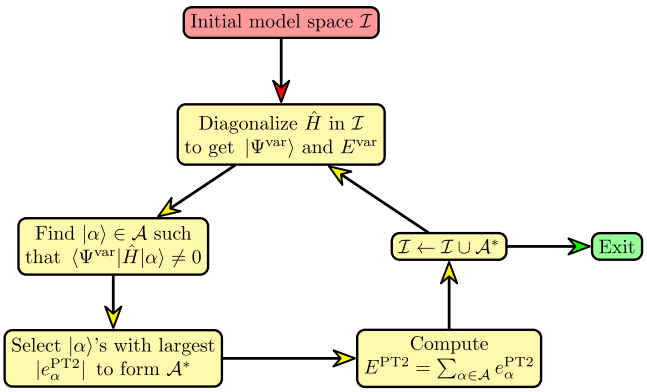

Figure 1. Iterative procedure followed by the CIPSI algorithm in the case of a single-state calculation. See ref 171 for a description of the multistate version.

In the case of a globally neutral system, the dipole operator is

$$\hat{\boldsymbol{\mu}} = -\sum_i \boldsymbol{r}_i + \sum_A Z_A \boldsymbol{R}_A \tag{8}$$

and the dipole moment computed from the zeroth-order wave function associated with the kth state is consequently

$$\boldsymbol{\mu}_k = \langle\Psi_k^{\mathrm{var}}|\hat{\boldsymbol{\mu}}|\Psi_k^{\mathrm{var}}\rangle = -\sum_i \langle\Psi_k^{\mathrm{var}}|\boldsymbol{r}_i|\Psi_k^{\mathrm{var}}\rangle + \sum_A Z_A \boldsymbol{R}_A \tag{9}$$

while the oscillator strength computed in the so-called length representation is given by

$$f_k^{\mathrm{L}} = \frac{2\Delta E_k^{\mathrm{var}}}{3}\boldsymbol{\lambda}_k\cdot\boldsymbol{\lambda}_k \tag{10}$$

where

$$\boldsymbol{\lambda}_k = -\sum_i \langle\Psi_0^{\mathrm{var}}|\boldsymbol{r}_i|\Psi_k^{\mathrm{var}}\rangle \tag{11}$$

is the transition dipole moment and $\Delta E_k^{\mathrm{var}} = E_k^{\mathrm{var}} - E_0^{\mathrm{var}}$ is the vertical excitation energy associated with the kth excited state. It is also possible to compute the oscillator strength in the velocity representation. In this case, it reads

$$f_k^{\mathrm{V}} = \frac{2}{3\Delta E_k^{\mathrm{var}}}\boldsymbol{\nu}_k\cdot\boldsymbol{\nu}_k \tag{12}$$

where

$$\boldsymbol{\nu}_k = -\sum_i \langle\Psi_0^{\mathrm{var}}|\boldsymbol{p}_i|\Psi_k^{\mathrm{var}}\rangle \tag{13}$$

and $\boldsymbol{p}_i = -\mathrm{i}\nabla_i$ is the momentum operator of electron i. It is also useful to compute the mixed length−velocity representation

$$f_k^{\mathrm{LV}} = -\frac{2\mathrm{i}}{3}\boldsymbol{\mu}_k\cdot\boldsymbol{\nu}_k \tag{14}$$

which does not involve the energy difference between the two electronic states. The quantities $\boldsymbol{\mu}_k$, $\boldsymbol{\lambda}_k$, and $\boldsymbol{\nu}_k$ defined in eqs 9, 11, and 13 are easily computed using the Slater−Condon rules.[11,172]

For practical purposes, it is convenient to recast eq 9 as

$$\boldsymbol{\mu}_k = -\sum_{pq}\gamma_{pq}^k\langle\phi_p|\boldsymbol{r}|\phi_q\rangle + \sum_A Z_A\boldsymbol{R}_A \tag{15}$$

where

$$\gamma_{pq}^k = \langle\Psi_k^{\mathrm{var}}|\hat{a}_q^\dagger\hat{a}_p|\Psi_k^{\mathrm{var}}\rangle \tag{16}$$

are the elements of the one-electron density matrix associated with the kth state, and $\hat{a}_p^\dagger$ ($\hat{a}_p$) is the second quantization creation (annihilation) operator that creates (annihilates) an electron in the spatial orbital $\phi_p(\boldsymbol{r})$. Similarly, for the oscillator strengths, $\boldsymbol{\nu}_k$ and $\boldsymbol{\lambda}_k$ can be computed with the one-electron transition density matrix, $\boldsymbol{\gamma}^{0k}$, as follows

$$\boldsymbol{\nu}_k = -\sum_{pq}\gamma_{pq}^{0k}\langle\phi_p|\boldsymbol{r}|\phi_q\rangle \tag{17a}$$

$$\boldsymbol{\lambda}_k = -\sum_{pq}\gamma_{pq}^{0k}\langle\phi_p|\boldsymbol{p}|\phi_q\rangle \tag{17b}$$

with

$$\gamma_{pq}^{0k} = \langle\Psi_0^{\mathrm{var}}|a_q^\dagger a_p|\Psi_k^{\mathrm{var}}\rangle \tag{18}$$

III. COMPUTATIONAL DETAILS

The molecules and states considered in this paper are represented in Figure 2. The geometries (computed at the

B−H	$^1\Sigma^+$, $^1\Pi$	$H_2C{=}O$	$^1A_1$, $^1A_2$
Cl−H	$^1\Sigma^+$, $^1\Pi$	$H_2C{=}S$	$^1A_1$, $^1A_2$
	$^1A_1$, $^1B_1$, $^1A_2$, $^1A_1$		$^1A'$, $^1A''$
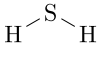	$^1A_1$, $^1A_2$, $^1B_1$	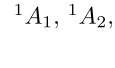	$^1A'$, $^1A''$
B−F	$^1A_1$, $^1\Pi$	$H_2C{=}Si$	$^1A_1$, $^1A_2$, $^1B_2$
C≡O	$^1\Sigma^+$, $^1\Pi$		

Figure 2. List of molecules and states studied in the present study.

CC3/aug-cc-pVTZ level) and the CC results reported here have been taken from the work of Chrayteh et al.[140] All these calculations have been performed within the frozen (large for third-row atoms) core approximation with the MRCC software.[173] For the sake of completeness, these geometries as well as the corresponding HF energies in the different basis sets are reported in the Supporting Information. Here, we consider only singlet−singlet transitions, but the same procedure can be employed for higher spin states.

Concerning the properties, the CC dipole moments have been computed within the LR formalism and are the so-called "orbital-relaxed" ones, which are known to be more accurate as the orbital response is properly taken into account. The SCI oscillator strengths have been computed in the length, velocity, and mixed representations, while their CC counterparts are available only in the length representation. All the SCI+PT2 calculations have been performed with QUANTUM PACKAGE,[37] where the CIPSI algorithm (see Selected Configuration Interaction) is implemented and where we have implemented the calculation of dipole moments and oscillator strengths at the SCI level using the expectation value formalism presented in Properties as Expectation Values. The raw data associated with each figure and table can be found in the Supporting Information.

https://doi.org/10.1021/acs.jctc.2c01111
J. Chem. Theory Comput. 2023, 19, 221−234

Table 1. Dipole Moment of 26 Electronic States and Oscillator Strengths in the Length (L), Velocity (V), and Mixed (LV) Representations for the 9 Dipole-Allowed Transitions Computed at the exFCI/aug-cc-pVTZ Level[a]

			exFCI				TBE	
molecule	excitation	nature	$\|\|\mu\|\|$	f^{L}	f^{V}	f^{LV}	$\|\|\mu\|\|$	f^{L}
BH	$^1\Sigma^+$		1.408(0)				1.409	
	$^1\Pi$	V	0.554(0)	0.048(0)	0.057(0)	0.052(0)	0.559	0.048
HCl	$^1\Sigma^+$		1.084(0)				1.084	
	$^1\Pi$	V	2.501(0)	0.055(0)	0.054(0)	0.054(0)	2.501	0.055
H_2O	$^1A_1$		1.840(0)				1.840	
	$^1B_1(n \rightarrow 3s)$	R	1.558(0)	0.054(0)	0.056(0)	0.055(0)	1.558	0.054
	$^1A_2(n \rightarrow 3p)$	R	1.105(1)				1.106	
	$^1A_1(n \rightarrow 3s)$	R	1.214(1)	0.100(0)	0.102(0)	0.101(0)	1.213	0.100
H_2S	$^1A_1$		0.977(0)				0.977	
	$^1A_2(n \rightarrow 4p)$	R	0.499(1)				0.498	
	$^1B_1(n \rightarrow 4s)$	R	1.866(1)	0.063(0)	0.063(0)	0.063(0)	1.865	0.063
BF	$^1A_1$		0.824(1)				0.824	
	$^1\Pi_1(\sigma \rightarrow \pi^*)$	V	0.294(1)	0.468(0)	0.490(1)	0.479(0)	0.299	0.468
CO	$^1\Sigma_1$		0.116(1)				0.115	
	$^1\Pi_1(n \rightarrow \pi^*)$	V	0.130(0)	0.166(0)	0.173(0)	0.170(1)	0.126	0.166
H_2CO	$^1A_1$		2.384(5)				2.375	
	$^1A_2(n \rightarrow \pi^*)$	V	1.325(2)				1.325	
H_2CS	$^1A_1$		1.695(3)				1.694	
	$^1A_2(n \rightarrow \pi^*)$	V	0.839(6)				0.840	
HNO	$^1A'$		1.676(1)				1.674	
	$^1A''(n \rightarrow \pi^*)$	V	1.675(3)				1.676	
FCH	$^1A'$		1.439(2)				1.438	
	$^1A''$	V	0.958(5)	0.006(0)	0.008(0)	0.007(0)	0.964	0.006
H_2CSi	$^1A_1$		0.137(3)				0.142	
	$^1A_2$	R	1.933(2)				1.924	
	$^1B_2$	R	0.042(1)	0.034(1)	0.032(0)	0.033(0)	0.039	0.034

[a]The TBEs extracted from the work of Chrayteh et al.[140] and computed in the same basis are also listed. An estimate of the extrapolation error associated with each value is reported in parentheses. V and R stand for valence and Rydberg excited states, respectively.

For each system, starting from the HF orbitals, a first multistate SCI calculation is performed to generate wave functions with at least 5×10^6 determinants, or large enough to reach a PT2 energy smaller than 1×10^{-6} E_h. These wave functions are then used to generate state-averaged natural orbitals. For the smallest molecules (BH, HCl, H_2O, H_2S, and BF), state-averaged optimized orbitals have been computed starting from these state-averaged natural orbitals via minimization of the variational energy at each CIPSI iteration until reaching at least 2×10^5 determinants or an energy gain between two successive iterations smaller than 1×10^{-6} E_h. More details about the orbital optimization in SCI can be found in refs 48 and 49. For the remaining larger systems, we did not see any improvement going from natural to optimized orbitals. Consequently, the calculations on the second set of molecules have been performed using the state-averaged natural orbitals. Our goal is to reach a variational space with at least 5×10^7 determinants or large enough to reach a PT2 energy smaller than 1×10^{-6} E_h. The energies, dipole moments, and oscillator strengths are computed at each CIPSI iteration using the variational wave function and are extrapolated to the FCI limit, i.e., $E_k^{PT2} \rightarrow 0$, by fitting a second-degree polynomial using the last 4 points, i.e., corresponding to the four largest variational wave functions (see Extrapolation Procedure for additional details about the extrapolation procedure). We refer to these results as extrapolated FCI (exFCI) values in the following. Note that excitation energies are computed as differences of extrapolated (total) energies.[42,44,174−179]

In the statistical analysis presented below, we report the usual indicators: the mean signed error (MSE), the mean absolute error (MAE), the root-mean-square error (RMSE), the standard deviation of the errors (SDE), as well as the largest positive and negative deviations [Max(+) and Max(−), respectively].

IV. RESULTS AND DISCUSSION

The dipole moments of the 26 states investigated in the present study alongside the oscillator strengths (in the length, velocity, and mixed representations) of the 9 dipole-allowed electronic transitions are listed in Table 1. We also report in parentheses an estimate of the extrapolation error associated with each value (see below). The TBEs taken from the work of Chrayteh et al.[140] are listed as well.

IV.A. Extrapolation Procedure. As discussed above, in the CIPSI method, the wave function is built iteratively. At each iteration, the determinants with the largest contributions to the second-order perturbative energy, $|e_\alpha^{PT2}|$, are added to the variational space (see Figure 1). In practice, we double the size of the variational space at each iteration and include the additional determinants required to obtain eigenstates of the $\hat{S}^2$ spin operator.[180] As a consequence of this growth, the variational energy decreases as the number of iterations

https://doi.org/10.1021/acs.jctc.2c01111
J. Chem. Theory Comput. 2023, 19, 221−234

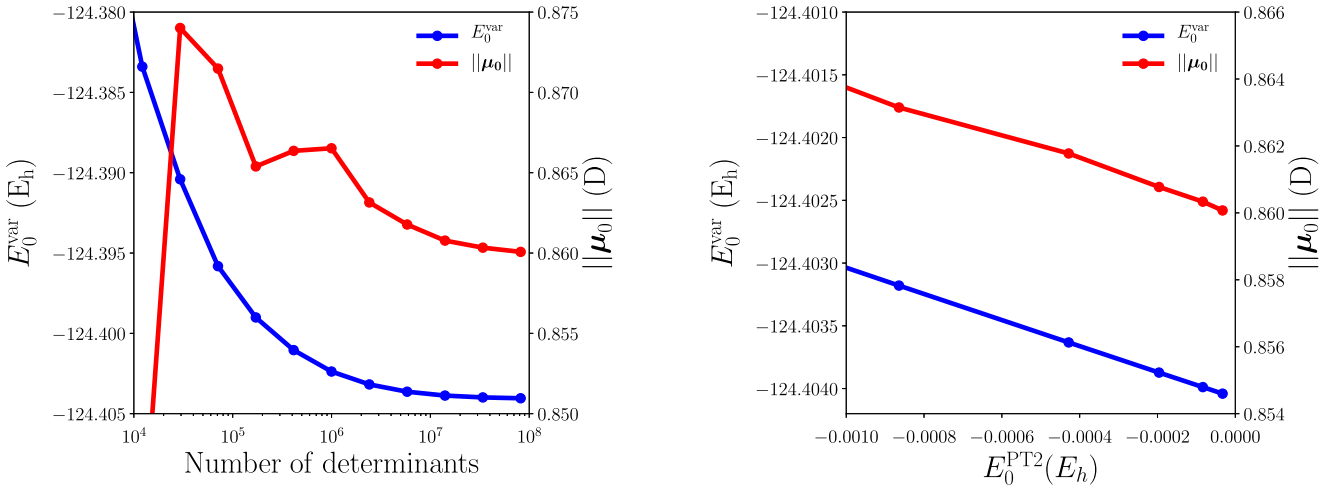

Figure 3. Ground-state variational energy E_0^{var} of BF (obtained with the aug-cc-pVDZ basis) and its corresponding dipole moment $||\boldsymbol{\mu}_0||$ as functions of the number of determinants in the variational wave function (left) and the second-order perturbative energy E_0^{PT2} (right).

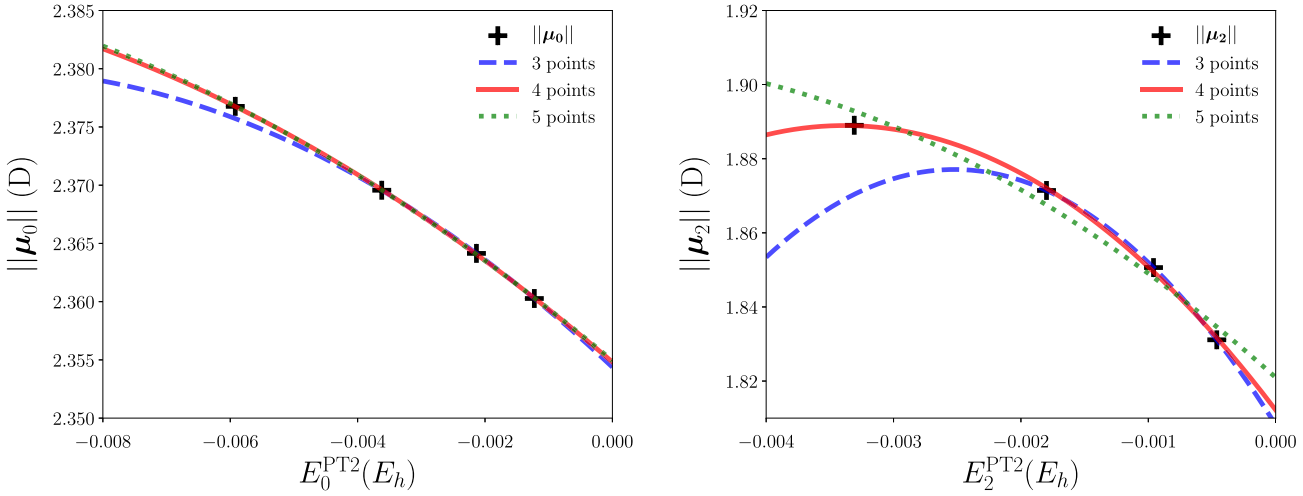

Figure 4. Left: Ground-state dipole moment of H_2C = O (obtained with the aug-cc-pVDZ basis), $||\boldsymbol{\mu}_0||$, as a function of the second-order perturbative energy E_0^{PT2}. Right: Second excited-state dipole moment of H_2S (obtained with the aug-cc-pVQZ basis), $||\boldsymbol{\mu}_2||$, as a function of the second-order energy E_2^{PT2}. The corresponding quadratic fits obtained with 3, 4, and 5 points are also reported. The raw data associated with these extrapolations can be found in Table 2.

increases. This is, of course, not strictly true for properties that are not directly linked to the variational principle. However, even if there is no direct relationship between the quality of the variational energy and a given property, the important determinants for the description of this property will eventually enter the variational space as it grows. Consequently, although it is possible to directly select determinants for a given property as shown by Angeli and co-workers,[181] the determinant selection based on an energy criterion is, in practice, a reasonable and universal way of producing accurate properties at the SCI level.

To illustrate these points, we report in the left panel of Figure 3 the evolution of the ground-state variational energy E_0^{var} and the norm of the ground-state dipole moment $||\boldsymbol{\mu}_0||$ as functions of the number of determinants in the variational space for the BF molecule computed in the aug-cc-pVDZ basis. As one can see, while E_0^{var} decreases monotonically toward the FCI limit (blue curve), the convergence of $||\boldsymbol{\mu}_0||$ (red curve) is more erratic but $||\boldsymbol{\mu}_0||$ eventually stabilizes for large enough wave functions and converges smoothly to its FCI limiting value.

To have a closer look at the region where one performs the extrapolation, we have plotted in the right panel of Figure 3 the evolution of the same quantities (for the same system) as functions of the second-order perturbative energy $E_0^{(2)}$. As empirically observed, the behavior of E_0^{var} for small E_0^{PT2} is linear as expected from basic perturbative arguments (see blue curve in Figure 3). One can therefore safely extrapolate E_0^{var} to $E_0^{\mathrm{PT2}} = 0$ using the largest variational wave functions (or equivalently the smallest E_0^{PT2} values) using a first- or second-order polynomial in E_0^{PT2} to estimate the FCI energy. A similar observation holds for the dipole moment (red curve), but the corresponding curve shows a significant quadratic character and the asymptotic regime usually appears for larger wave functions (see below). Nonetheless, we employ the same procedure as for the energy and estimate the FCI value of the dipole moment using a quadratic fit in E_0^{PT2} based on the four

https://doi.org/10.1021/acs.jctc.2c01111
J. Chem. Theory Comput. 2023, 19, 221−234

largest variational wave functions. A rough error estimate is provided by the largest difference in extrapolated values between this 4-point fit and its 3- and 5-point counterparts.

This procedure is performed independently for each electronic state in the case of the energy and the dipole moment. For the oscillator strength that is naturally related to the ground and the target excited state, the extrapolation procedure involves a second-order polynomial in the averaged second-order perturbative energies $(E_0^{PT2} + E_k^{PT2})/2$.

Illustrative examples for dipole moments are reported in Figure 4 and the corresponding numerical values are gathered in Table 2. The left panel of Figure 4 shows a well-behaved case where the data are fitted quite well by a quadratic polynomial and the extrapolated value is fairly independent of the number of points. The right panel shows an ill-behaved case where our procedure can hardly model the evolution of the dipole moment and the error is of the order of 0.01 D. Problematic cases are hard to detect *a priori* and depend on the selected system, state, and basis set.

Table 2. Dipole Moments of the Ground State of $H_2C = O$ Obtained at the exFCI/aug-cc-pVDZ Level and the Second Excited State of H_2S Obtained at the exFCI/aug-cc-pVQZ Level as Functions of the Number of Points Included in the Extrapolation Procedure[a]

	$H_2C = O$		H_2S	
number of points	$\|\boldsymbol{\mu}_0\|$ (D)	Δ (D)	$\|\boldsymbol{\mu}_2\|$ (D)	Δ (D)
3	2.3544	0.0004	1.8082	0.0040
4	2.3548		1.8122	
5	2.3549	0.0001	1.8210	0.0088

[a]Δ is the deviation to the four-point extrapolation.

Figure 5 reports the oscillator strength between the ground and first excited states of H_2S computed with the aug-cc-pVDZ basis set, in the length, velocity, and mixed representations. In the case of oscillator strengths, we also rely on quadratic fits to estimate the FCI limiting values and the corresponding fitting errors. The different limiting values reached with the three representations are clearly visible in the left panel. We underline that these differences remain fairly small (below 10^{-3} in this particular case). The right panel shows the extrapolation (with different numbers of points) of f_1^L as a function of $(E_0^{PT2} + E_1^{PT2})/2$.

IV.B. Dipole Moments. Our goal is to gauge the quality of the (orbital-relaxed) dipole moments obtained at various LR-CC levels for our set of 11 molecules, by comparing them to our near-FCI estimates. The box plot representations of the error in ground- and excited-state dipole moments computed at the CCSD (blue), CCSDT (red), and CCSDTQ (green) levels for all basis sets listed in the Supporting Information are represented in Figure 6. The corresponding statistical quantities are reported in Table 3. We decided not to report any trends on CCSDTQP as the error between the latter method and exFCI is of the same order of magnitude as the extrapolation errors.

Considering both the ground- and excited-state dipoles, the usual trend of systematic improvement is nicely illustrated with the MAEs going down from 4.5×10^{-2} D for CCSD to 1.8×10^{-3} D for CCSDTQ. The inclusion of triples already provides an accuracy below 10^{-2} D (MAE of 9.1×10^{-3} D for CCSDT), which would be classified as very accurate for most applications. In other words, going from one excitation degree to the next one (from CCSD to CCSDT or from CCSDT to CCSDTQ) reduces most of the statistical indicators by approximately 1 order of magnitude. The MSEs are positive for both ground and excited states, meaning that the magnitudes of the dipole moments tend to be overestimated by LR-CC, at least for the present set of compounds. In addition, the largest errors are generally positive and obtained for the excited-state dipoles. An analysis of the other statistical quantities leads to similar conclusions. As one notices by comparing the central and right panels of Figure 6, CC methods are more accurate for ground-state dipole moments than for excited-state ones, which is expected since the LR (as well as EOM) formalism is naturally biased toward the ground state.

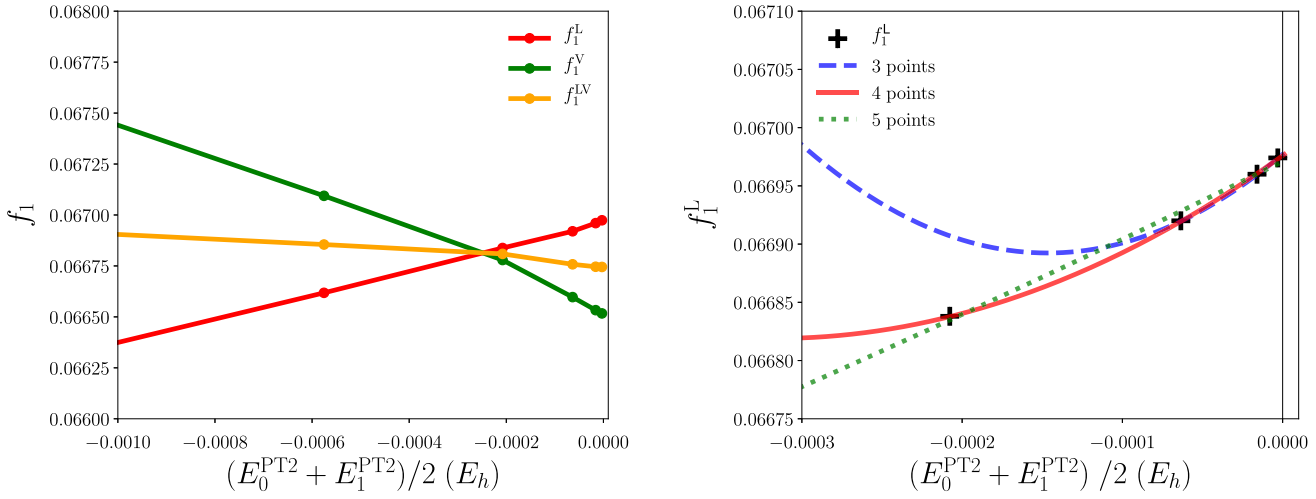

Figure 5. Oscillator strength of H_2S for the transition between the ground and lowest excited state (obtained with the aug-cc-pVDZ basis), f_1, in the length (L), velocity (V), and mixed (LV) representations, as a function of the averaged second-order perturbative energies $(E_0^{PT2} + E_1^{PT2})/2$. For the length representation, a zoomed-in view of the region where the extrapolation is performed is shown in the right panel. The corresponding quadratic fits obtained with 3, 4, and 5 points are also reported.

https://doi.org/10.1021/acs.jctc.2c01111
J. Chem. Theory Comput. 2023, 19, 221−234

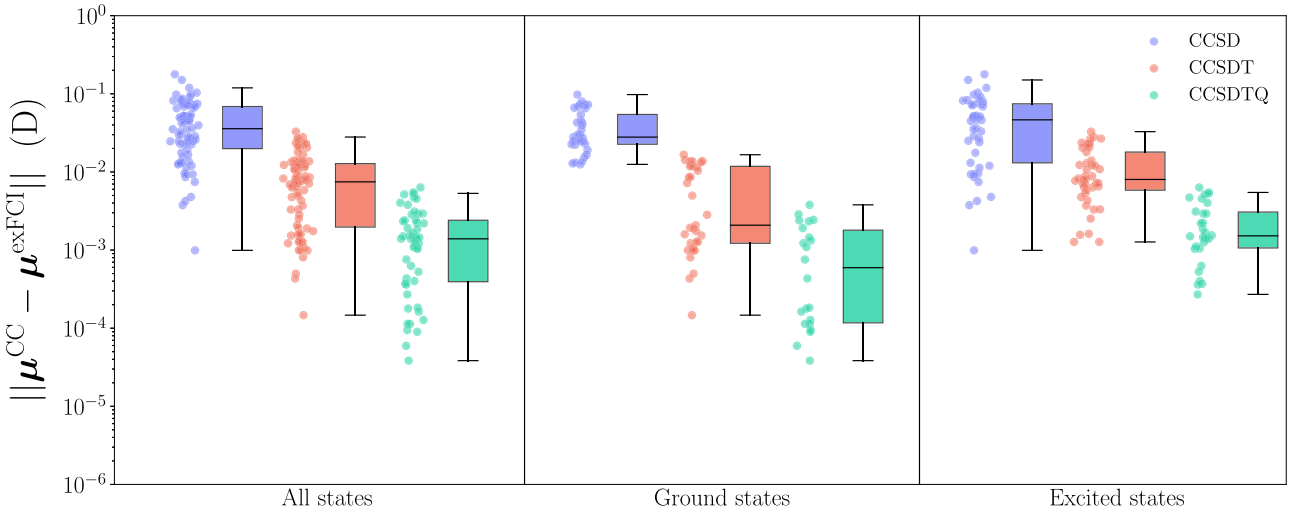

Figure 6. Box plots of the error in the ground- and excited-state dipole moments (with respect to exFCI) obtained with the CCSD (blue), CCSDT (red), and CCSDTQ (green) levels for all basis sets listed in the Supporting Information.

Table 3. Statistical Measures Associated with the Errors (with Respect to exFCI) of Ground-State (GS) and Excited-State (ES) Dipole Moments Computed at the CCSD, CCSDT, and CCSDTQ Levels for All Basis Sets Listed in the Supporting Information

			statistical quantities (in D)					
method	state	# states	MSE	MAE	SDE	RMSE	Max(+)	Max(−)
CCSD	All	78	1.3×10^{-2}	4.5×10^{-2}	5.5×10^{-2}	5.7×10^{-2}	1.5×10^{-1}	-1.8×10^{-1}
	GS	33	2.2×10^{-2}	3.8×10^{-2}	3.9×10^{-2}	4.5×10^{-2}	9.8×10^{-2}	-6.6×10^{-2}
	ES	45	6.8×10^{-3}	5.0×10^{-2}	6.3×10^{-2}	6.4×10^{-2}	1.5×10^{-1}	-1.8×10^{-1}
CCSDT	All	78	4.5×10^{-3}	9.1×10^{-3}	1.1×10^{-2}	1.2×10^{-2}	3.3×10^{-2}	-2.8×10^{-2}
	GS	33	3.7×10^{-3}	5.9×10^{-3}	7.1×10^{-3}	8.1×10^{-3}	1.7×10^{-2}	-1.2×10^{-2}
	ES	45	5.2×10^{-3}	1.1×10^{-2}	1.3×10^{-2}	1.4×10^{-2}	3.3×10^{-2}	-2.8×10^{-2}
CCSDTQ	All	52	8.9×10^{-4}	1.8×10^{-3}	2.2×10^{-3}	2.4×10^{-3}	5.3×10^{-3}	-6.3×10^{-3}
	GS	22	4.0×10^{-4}	1.1×10^{-3}	1.5×10^{-3}	1.5×10^{-3}	3.8×10^{-3}	-2.9×10^{-3}
	ES	30	1.3×10^{-3}	2.3×10^{-3}	2.6×10^{-3}	2.9×10^{-3}	5.3×10^{-3}	-6.3×10^{-3}

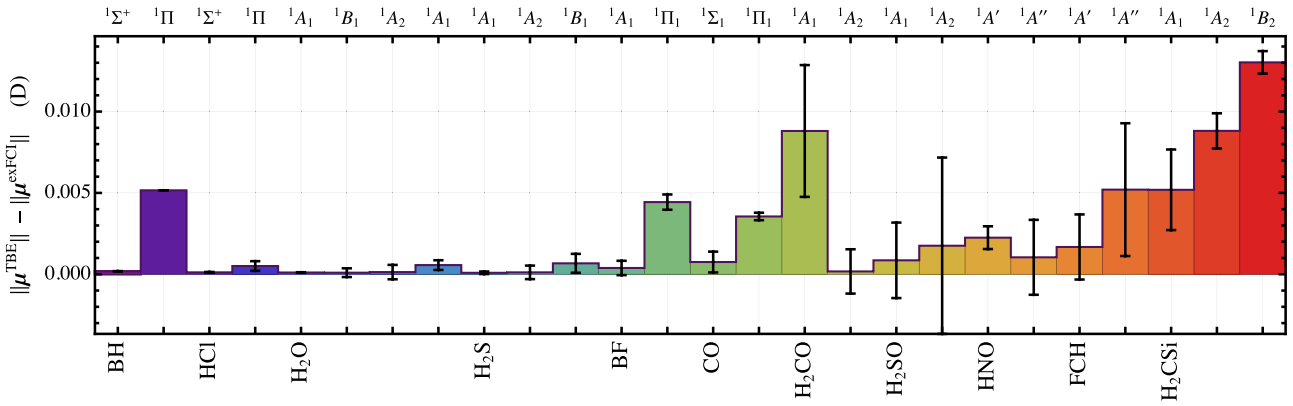

Figure 7. Comparison between the orbital-relaxed TBE dipole moments from Chrayteh et al.[140] and the present exFCI values for the 26 states considered in the present study. The estimated extrapolation error associated with each exFCI value is also reported. All these quantities have been computed in the aug-cc-pVTZ basis.

The exFCI/aug-cc-pVTZ values can also be compared to the orbital-relaxed TBEs obtained by Chrayteh et al.[140] for the dipole moments computed in the same basis. The differences between these two sets of accurate data are reported in Figure 7 (see Table 1 for the raw data). Small differences are observed for BH and BF between the orbital-relaxed and orbital-unrelaxed dipole moments of the first excited state due to the frozen core approximation (see Introduction).[132] For formaldehyde, fluorocarbene, and silylidene, the convergence of the CIPSI calculations for the different states is not completely satisfactory, leading to larger uncertainties on the exFCI values, hence explaining the difference with the TBEs. Excluding these cases, the TBEs are found to be in excellent agreement with the exFCI results with differences of a few mD only.

C. Oscillator Strengths. Let us now focus on the performance of CC methods for oscillator strengths by

https://doi.org/10.1021/acs.jctc.2c01111
J. Chem. Theory Comput. 2023, 19, 221−234

Table 4. Statistical Measures Associated with the Errors (with Respect to exFCI) of the Oscillator Strengths Computed in the Length Representation at the CCSD, CCSDT, and CCSDTQ Levels for All Basis Sets Listed in the Supporting Information

		statistical quantities					
method	# states	MSE	MAE	SDE	RMSE	Max(+)	Max(−)
CCSD	27	5.0×10^{-4}	2.4×10^{-3}	3.2×10^{-3}	3.2×10^{-3}	7.1×10^{-3}	-7.2×10^{-3}
CCSDT	27	-1.6×10^{-4}	4.1×10^{-4}	6.1×10^{-4}	6.3×10^{-4}	6.8×10^{-4}	-1.9×10^{-3}
CCSDTQ	18	-4.4×10^{-5}	7.0×10^{-5}	1.2×10^{-4}	1.3×10^{-4}	8.9×10^{-5}	-3.8×10^{-4}

comparing them to exFCI. The corresponding statistical analysis considering length representation (for all basis sets listed in the Supporting Information) can be found in Table 4. The box plots of the errors associated with CCSD, CCSDT, and CCSDTQ are represented in Figure 8.

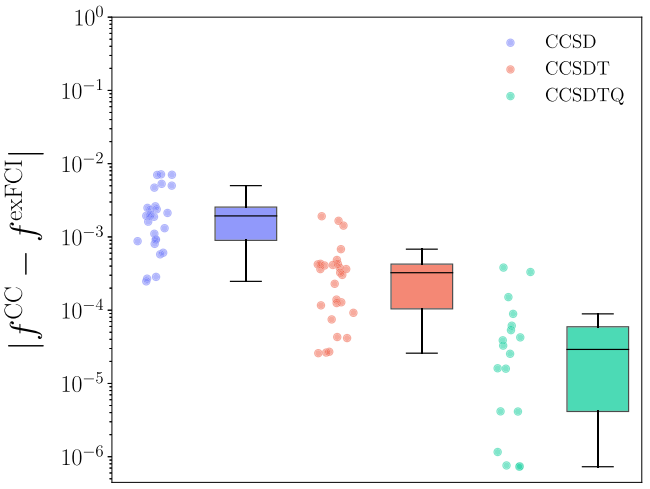

Figure 8. Box plots of the error in oscillator strengths (with respect to exFCI) computed at the CCSD (blue), CCSDT (red), and CCSDTQ (green) levels for various basis sets.

Concerning the statistics, the results gathered in Table 4 show that the MSEs of the different CC methods are close to zero, sometimes positive and sometimes negative, meaning that one cannot conclude if the oscillator strengths tend to be overestimated or underestimated. Also, similarly to the dipole moments, going from one excitation degree to the next one reduces the error and all the statistical quantities by approximately 1 order of magnitude (see Figure 8). Overall, we have found that the oscillator strengths are easier to converge at the SCI level than the individual dipole moments. We note that CCSDT provides a MAE well below 10^{-3}, which is sufficient for most applications.

Table 1 reports the oscillator strengths at the exFCI/aug-cc-pVTZ level in the different representations for the 9 dipole-allowed transitions considered in the present study. The corresponding TBEs extracted from the work of Chrayteh et al.[140] and computed in the length representation are also listed for comparison purposes. As one would see, there is a perfect agreement between the two sets of data, which confirms the quality of the TBEs reported in ref 140. In Table 1, we also report the oscillator strengths computed in the velocity and mixed representations. Except for a few valence transitions, they do not significantly differ from their length counterparts. In each case, f^{LV} can be fairly well approximated by the averaged value of f^{L} and f^{V}, as expected from their mathematical definitions (see Properties as Expectation Values).

V. CONCLUDING REMARKS

In this work, we have implemented the computation of the ground- and excited-state dipole moments, as well as the oscillator strengths, at the SCI level using the expectation value formalism. Thanks to an efficient implementation of the SCI +PT2 method known as CIPSI and tailored extrapolation procedures, we have been able to reach near-FCI accuracy for these properties in the case of 11 small molecules. In most cases, the magnitude of the dipole moments was computed with an accuracy of a few mD. Similarly, we have reached an accuracy of the order of 10^{-4} for the oscillator strengths in the length, velocity, and mixed representations. Of course, the accuracy is constrained by the size of the Hilbert space, and reaching such a level of precision is hence limited to compact systems. Nevertheless, the principal ambitions of the present work are to illustrate (i) how one can reach near-FCI quality for electronic properties with SCI+PT2 methods and (ii) how they can be useful to estimate errors in state-of-the-art CC models which are usually challenging to assess due to the lack of reference data. The main highlights of the present benchmark are that CCSDT is accurate enough for most practical applications, while CCSD produces MAEs of 3.8×10^{-2} D (5.0×10^{-2} D) and 2.4×10^{-3} for ground-state (excited-state) dipole moments and oscillator strengths, respectively.

As a perspective, the present strategy could be further improved by taking into account the (perturbative) first-order wave function in the computation of the expectation values. This would be particularly useful to tackle larger systems. Work along these lines is currently in progress in our group.

■ ASSOCIATED CONTENT

Supporting Information

The Supporting Information is available free of charge at https://pubs.acs.org/doi/10.1021/acs.jctc.2c01111.

Raw data associated with each figure and table, the molecular geometries, and the Hartree−Fock energies corresponding to the different basis sets (TXT)

Dipole moments and oscillator strengths of the 11 molecules for all levels of theory and basis sets considered in the paper (PDF)

■ AUTHOR INFORMATION

Corresponding Authors

Yann Damour − *Laboratoire de Chimie et Physique Quantiques (UMR 5626), Université de Toulouse, CNRS, UPS, 31062 Toulouse, France*; Email: yann.damour@irsamc.ups-tlse.fr

Pierre-François Loos − *Laboratoire de Chimie et Physique Quantiques (UMR 5626), Université de Toulouse, CNRS, UPS, 31062 Toulouse, France*; orcid.org/0000-0003-0598-7425; Email: loos@irsamc.ups-tlse.fr

https://doi.org/10.1021/acs.jctc.2c01111
J. Chem. Theory Comput. 2023, 19, 221−234

Authors

Raúl Quintero-Monsebaiz − *Laboratoire de Chimie et Physique Quantiques (UMR 5626), Université de Toulouse, CNRS, UPS, 31062 Toulouse, France*

Michel Caffarel − *Laboratoire de Chimie et Physique Quantiques (UMR 5626), Université de Toulouse, CNRS, UPS, 31062 Toulouse, France*

Denis Jacquemin − *Nantes Université, CNRS, CEISAM UMR 6230, F-44000 Nantes, France; Institut Universitaire de France (IUF), F-75005 Paris, France;* orcid.org/0000-0002-4217-0708

Fábris Kossoski − *Laboratoire de Chimie et Physique Quantiques (UMR 5626), Université de Toulouse, CNRS, UPS, 31062 Toulouse, France;* orcid.org/0000-0002-1627-7093

Anthony Scemama − *Laboratoire de Chimie et Physique Quantiques (UMR 5626), Université de Toulouse, CNRS, UPS, 31062 Toulouse, France;* orcid.org/0000-0003-4955-7136

Complete contact information is available at: https://pubs.acs.org/10.1021/acs.jctc.2c01111

Notes

The authors declare no competing financial interest.

■ ACKNOWLEDGMENTS

This project has received funding from the European Research Council (ERC) under the European Union's Horizon 2020 research and innovation programme (Grant Agreement No. 863481). This work used the HPC resources from CALMIP (Toulouse) under allocation 2022-18005 and from the CCIPL center (Nantes).

■ REFERENCES

(1) Minkin, V. I.; Osipov, O. A.; Zhdanov, Y. A. *Dipole Moments in Organic Chemistry*; Springer US, 1970.

(2) Bergmann, E.; Weizmann, A. Dipole Moments as a Tool in the Determination of Structure. *Chem. Rev.* **1941**, *29*, 553−592.

(3) Laubengayer, A. W.; Rysz, W. R. The Dipole Moments of the Isomers of Dicarbadecaborane, B10H10C2H2. *Inorg. Chem.* **1965**, *4*, 1513−1514.

(4) Skoog, D. A.; Holler, F. J.; Crouch, S. R. *Principles of Instrumental Analysis*; Cengage Learning, 2006.

(5) Nikitin, A. V.; Rey, M.; Tyuterev, V. G. New dipole moment surfaces of methane. *Chem. Phys. Lett.* **2013**, *565*, 5−11.

(6) Diehr, M.; Rosmus, P.; Carter, S.; Knowles, P. J. Theoretical rovibrational line intensities in the electronic ground state of ozone. *Mol. Phys.* **2004**, *102*, 2181−2189.

(7) Tyuterev, V. G.; Kochanov, R. V.; Tashkun, S. A. Accurate ab initio dipole moment surfaces of ozone: First principle intensity predictions for rotationally resolved spectra in a large range of overtone and combination bands. *J. Chem. Phys.* **2017**, *146*, 064304.

(8) Hait, D.; Head-Gordon, M. How Accurate Is Density Functional Theory at Predicting Dipole Moments? An Assessment Using a New Database of 200 Benchmark Values. *J. Chem. Theory Comput.* **2018**, *14*, 1969−1981.

(9) Giner, E.; Traore, D.; Pradines, B.; Toulouse, J. Self-consistent density-based basis-set correction: How much do we lower total energies and improve dipole moments? *J. Chem. Phys.* **2021**, *155*, 044109.

(10) Gupta, V. P. 9 - Interaction of Radiation and Matter and Electronic Spectra. *Principles and Applications of Quantum Chemistry* **2016**, 291−337.

(11) Szabo, A.; Ostlund, N. S. *Modern quantum chemistry*; McGraw-Hill: New York, 1989.

(12) Helgaker, T.; Jørgensen, P.; Olsen, J. *Molecular Electronic-Structure Theory*; John Wiley & Sons, Inc., 2013.

(13) Jensen, F. *Introduction to Computational Chemistry*, 3rd ed.; Wiley: Hoboken, NJ, USA, 2017.

(14) Yoshimine, M.; Mclean, A. D. Ground states of linear molecules: Dissociation energies and dipole moments in the hartree−fock approximation. *Int. J. Quantum Chem.* **1967**, *1*, 313−326.

(15) Knowles, P. J.; Handy, N. C. A new determinant-based full configuration interaction method. *Chem. Phys. Lett.* **1984**, *111*, 315−321.

(16) Olsen, J.; Roos, B. O.; Jørgensen, P.; Jensen, H. J. Aa. Determinant based configuration interaction algorithms for complete and restricted configuration interaction spaces. *J. Chem. Phys.* **1988**, *89*, 2185−2192.

(17) Knowles, P. J.; Handy, N. C. A Determinant Based Full Configuration Interaction Program. *Comput. Phys. Commun.* **1989**, *54*, 75−83.

(18) Olsen, J.; Jørgensen, P.; Simons, J. Passing the one-billion limit in full configuration-interaction (FCI) calculations. *Chem. Phys. Lett.* **1990**, *169*, 463−472.

(19) Eriksen, J. J. The Shape of Full Configuration Interaction to Come. *J. Phys. Chem. Lett.* **2021**, *12*, 418−432.

(20) Ring, P.; Schuck, P. *The Nuclear Many-Body Problem*; Springer, 1980.

(21) Bytautas, L.; Henderson, T. M.; Jiménez-Hoyos, C. A.; Ellis, J. K.; Scuseria, G. E. Seniority and orbital symmetry as tools for establishing a full configuration interaction hierarchy. *J. Chem. Phys.* **2011**, *135*, 044119.

(22) Kossoski, F.; Damour, Y.; Loos, P.-F. Hierarchy Configuration Interaction: Combining Seniority Number and Excitation Degree. *J. Phys. Chem. Lett.* **2022**, *13*, 4342−4349.

(23) Bender, C. F.; Davidson, E. R. Studies in Configuration Interaction: The First-Row Diatomic Hydrides. *Phys. Rev.* **1969**, *183*, 23−30.

(24) Huron, B.; Malrieu, J. P.; Rancurel, P. Iterative perturbation calculations of ground and excited state energies from multiconfigurational zeroth-order wavefunctions. *J. Chem. Phys.* **1973**, *58*, 5745−5759.

(25) Buenker, R. J.; Peyerimhoff, S. D. Individualized configuration selection in CI calculations with subsequent energy extrapolation. *Theor. Chim. Acta* **1974**, *35*, 33−58.

(26) Evangelisti, S.; Daudey, J.-P.; Malrieu, J.-P. Convergence of an improved CIPSI algorithm. *Chem. Phys.* **1983**, *75*, 91−102.

(27) Angeli, C.; Cimiraglia, R. Multireference perturbation CI IV. Selection procedure for one-electron properties. *Theor. Chem. Acc.* **2001**, *105*, 259−264.

(28) Liu, W.; Hoffmann, M. R. iCI: Iterative CI toward full CI. *J. Chem. Theory Comput* **2016**, *12*, 1169−1178.

(29) Harrison, R. J. Approximating full configuration interaction with selected configuration interaction and perturbation theory. *J. Chem. Phys.* **1991**, *94*, 5021−5031.

(30) Giner, E.; Scemama, A.; Caffarel, M. Using perturbatively selected configuration interaction in quantum Monte Carlo calculations. *Can. J. Chem.* **2013**, *91*, 879−885.

(31) Holmes, A. A.; Tubman, N. M.; Umrigar, C. J. Heat-Bath Configuration Interaction: An Efficient Selected Configuration Interaction Algorithm Inspired by Heat-Bath Sampling. *J. Chem. Theory Comput.* **2016**, *12*, 3674−3680.

(32) Schriber, J. B.; Evangelista, F. A. Communication: An adaptive configuration interaction approach for strongly correlated electrons with tunable accuracy. *J. Chem. Phys.* **2016**, *144*, 161106.

(33) Tubman, N. M.; Lee, J.; Takeshita, T. Y.; Head-Gordon, M.; Whaley, K. B. A deterministic alternative to the full configuration interaction quantum Monte Carlo method. *J. Chem. Phys.* **2016**, *145*, 044112.

(34) Sharma, S.; Holmes, A. A.; Jeanmairet, G.; Alavi, A.; Umrigar, C. J. Semistochastic Heat-Bath Configuration Interaction Method:

Selected Configuration Interaction with Semistochastic Perturbation Theory. *J. Chem. Theory Comput.* **2017**, *13*, 1595−1604.
(35) Tubman, N. M.; Levine, D. S.; Hait, D.; Head-Gordon, M.; Whaley, K. B. An efficient deterministic perturbation theory for selected configuration interaction methods. *arXiv* **2018**, 1808.02049v1.
(36) Coe, J. P. Machine Learning Configuration Interaction. *J. Chem. Theory Comput.* **2018**, *14*, 5739−5749.
(37) Garniron, Y.; et al. Quantum Package 2.0: a open-source determinant-driven suite of programs. *J. Chem. Theory Comput.* **2019**, *15*, 3591.
(38) Zhang, N.; Liu, W.; Hoffmann, M. R. Iterative Configuration Interaction with Selection. *J. Chem. Theory Comput.* **2020**, *16*, 2296−2316.
(39) Giner, E.; Scemama, A.; Caffarel, M. Fixed-node diffusion Monte Carlo potential energy curve of the fluorine molecule F2 using selected configuration interaction trial wavefunctions. *J. Chem. Phys.* **2015**, *142*, 044115.
(40) Garniron, Y.; Scemama, A.; Loos, P.-F.; Caffarel, M. Hybrid Stochastic-Deterministic Calculation of the Second-Order Perturbative Contribution of Multireference Perturbation Theory. *J. Chem. Phys.* **2017**, *147*, 034101.
(41) Zhang, N.; Liu, W.; Hoffmann, M. R. Further Development of iCIPT2 for Strongly Correlated Electrons. *J. Chem. Theory Comput.* **2021**, *17*, 949−964.
(42) Holmes, A. A.; Umrigar, C. J.; Sharma, S. Excited states using semistochastic heat-bath configuration interaction. *J. Chem. Phys.* **2017**, *147*, 164111.
(43) Mussard, B.; Sharma, S. One-Step Treatment of Spin-Orbit Coupling and Electron Correlation in Large Active Spaces. *J. Chem. Theory Comput.* **2018**, *14*, 154−165.
(44) Chien, A. D.; Holmes, A. A.; Otten, M.; Umrigar, C. J.; Sharma, S.; Zimmerman, P. M. Excited States of Methylene, Polyenes, and Ozone from Heat-Bath Configuration Interaction. *J. Phys. Chem. A* **2018**, *122*, 2714−2722.
(45) Tubman, N. M.; Freeman, C. D.; Levine, D. S.; Hait, D.; Head-Gordon, M.; Whaley, K. B. Modern Approaches to Exact Diagonalization and Selected Configuration Interaction with the Adaptive Sampling CI Method. *J. Chem. Theory Comput.* **2020**, *16*, 2139−2159.
(46) Loos, P.-F.; Damour, Y.; Scemama, A. The performance of CIPSI on the ground state electronic energy of benzene. *J. Chem. Phys.* **2020**, *153*, 176101.
(47) Yao, Y.; Giner, E.; Li, J.; Toulouse, J.; Umrigar, C. J. Almost exact energies for the Gaussian-2 set with the semistochastic heat-bath configuration interaction method. *J. Chem. Phys.* **2020**, *153*, 124117.
(48) Damour, Y.; Véril, M.; Kossoski, F.; Caffarel, M.; Jacquemin, D.; Scemama, A.; Loos, P.-F. Accurate full configuration interaction correlation energy estimates for five- and six-membered rings. *J. Chem. Phys.* **2021**, *155*, 134104.
(49) Yao, Y.; Umrigar, C. J. Orbital Optimization in Selected Configuration Interaction Methods. *J. Chem. Theory Comput.* **2021**, *17*, 4183−4194.
(50) Larsson, H. R.; Zhai, H.; Umrigar, C. J.; Chan, G. K.-L. The Chromium Dimer: Closing a Chapter of Quantum Chemistry. *J. Am. Chem. Soc.* **2022**, *144*, 15932−15937.
(51) Coe, J. P.; Moreno Carrascosa, A.; Simmermacher, M.; Kirrander, A.; Paterson, M. J. Efficient Computation of Two-Electron Reduced Density Matrices via Selected Configuration Interaction. *J. Chem. Theory Comput.* **2022**, *18* (11), 6690−6699.
(52) Eriksen, J. J.; et al. The Ground State Electronic Energy of Benzene. *J. Phys. Chem. Lett.* **2020**, *11*, 8922−8929.
(53) Čížek, J. On the Correlation Problem in Atomic and Molecular Systems. Calculation of Wavefunction Components in Ursell-Type Expansion Using Quantum-Field Theoretical Methods. *J. Chem. Phys.* **1966**, *45*, 4256−4266.
(54) Čížek, J. *Advances in Chemical Physics*; John Wiley & Sons, Ltd: Chichester, England, UK, 1969; pp 35−89.
(55) Paldus, J. *Methods in Computational Molecular Physics*; Springer, Boston, MA: Boston, MA, USA, 1992; pp 99−194.
(56) Crawford, T. D.; Schaefer, H. F. *Reviews in Computational Chemistry*; John Wiley & Sons, Ltd: Chichester, England, UK, 2000; pp 33−136.
(57) Bartlett, R. J.; Musiał, M. Coupled-cluster theory in quantum chemistry. *Rev. Mod. Phys.* **2007**, *79*, 291−352.
(58) Shavitt, I.; Bartlett, R. J. *Many-Body Methods in Chemistry and Physics: MBPT and Coupled-Cluster Theory*; Cambridge University Press: Cambridge, England, UK, 2009.
(59) Purvis, G. P., III; Bartlett, R. J. A Full Coupled-Cluster Singles and Doubles Model: The Inclusion of Disconnected Triples. *J. Chem. Phys.* **1982**, *76*, 1910−1918.
(60) Scuseria, G. E.; Scheiner, A. C.; Lee, T. J.; Rice, J. E.; Schaefer, H. F. The closed-shell coupled cluster single and double excitation (CCSD) model for the description of electron correlation. A comparison with configuration interaction (CISD) results. *J. Chem. Phys.* **1987**, *86*, 2881−2890.
(61) Koch, H.; Jensen, H. J. A.; Jorgensen, P.; Helgaker, T. Excitation Energies from the Coupled Cluster Singles and Doubles Linear Response Function (CCSDLR). Applications to Be, CH^+, CO, and H_2O. *J. Chem. Phys.* **1990**, *93*, 3345−3350.
(62) Stanton, J. F.; Bartlett, R. J. The equation of motion coupled-cluster method. A systematic biorthogonal approach to molecular excitation energies, transition probabilities, and excited state properties. *J. Chem. Phys.* **1993**, *98*, 7029−7039.
(63) Stanton, J. F. Many-body methods for excited state potential energy surfaces. I. General theory of energy gradients for the equation-of-motion coupled-cluster method. *J. Chem. Phys.* **1993**, *99*, 8840−8847.
(64) Noga, J.; Bartlett, R. J. The Full CCSDT Model for Molecular Electronic Structure. *J. Chem. Phys.* **1987**, *86*, 7041−7050.
(65) Scuseria, G. E.; Schaefer, H. F. A new implementation of the full CCSDT model for molecular electronic structure. *Chem. Phys. Lett.* **1988**, *152*, 382−386.
(66) Watts, J. D.; Bartlett, R. J. The inclusion of connected triple excitations in the equation-of-motion coupled-cluster method. *J. Chem. Phys.* **1994**, *101*, 3073−3078.
(67) Kucharski, S. A.; Włoch, M.; Musiał, M.; Bartlett, R. J. Coupled-cluster theory for excited electronic states: The full equation-of-motion coupled-cluster single, double, and triple excitation method. *J. Chem. Phys.* **2001**, *115*, 8263−8266.
(68) Kucharski, S. A.; Bartlett, R. J. Recursive Intermediate Factorization and Complete Computational Linearization of the Coupled-Cluster Single, Double, Triple, and Quadruple Excitation Equations. *Theor. Chim. Acta* **1991**, *80*, 387−405.
(69) Kállay, M.; Surján, P. R. Higher excitations in coupled-cluster theory. *J. Chem. Phys.* **2001**, *115*, 2945−2954.
(70) Hirata, S. Higher-Order Equation-of-Motion Coupled-Cluster Methods. *J. Chem. Phys.* **2004**, *121*, 51−59.
(71) Kállay, M.; Gauss, J.; Szalay, P. G. Analytic first derivatives for general coupled-cluster and configuration interaction models. *J. Chem. Phys.* **2003**, *119*, 2991−3004.
(72) Kállay, M.; Gauss, J. Analytic second derivatives for general coupled-cluster and configuration-interaction models. *J. Chem. Phys.* **2004**, *120*, 6841−6848.
(73) Christiansen, O.; Koch, H.; Jørgensen, P. The Second-Order Approximate Coupled Cluster Singles and Doubles Model CC2. *Chem. Phys. Lett.* **1995**, *243*, 409−418.
(74) Hättig, C.; Weigend, F. CC2 Excitation Energy Calculations on Large Molecules Using the Resolution of the Identity Approximation. *J. Chem. Phys.* **2000**, *113*, 5154−5161.
(75) Christiansen, O.; Koch, H.; Jørgensen, P. Response Functions in the CC3 Iterative Triple Excitation Model. *J. Chem. Phys.* **1995**, *103*, 7429−7441.
(76) Koch, H.; Christiansen, O.; Jørgensen, P.; Olsen, J. Excitation Energies of BH, CH2 and Ne in Full Configuration Interaction and the Hierarchy CCS, CC2, CCSD and CC3 of Coupled Cluster Models. *Chem. Phys. Lett.* **1995**, *244*, 75−82.

(77) Koch, H.; Christiansen, O.; Jorgensen, P.; Sanchez de Merás, A. M.; Helgaker, T. The CC3Model: An Iterative Coupled Cluster Approach Including Connected Triples. *J. Chem. Phys.* **1997**, *106*, 1808−1818.
(78) Hald, K.; Jørgensen, P.; Olsen, J.; Jaszuński, M. An analysis and implementation of a general coupled cluster approach to excitation energies with application to the B2 molecule. *J. Chem. Phys.* **2001**, *115*, 671−679.
(79) Paul, A. C.; Myhre, R. H.; Koch, H. New and Efficient Implementation of CC3. *J. Chem. Theory Comput.* **2021**, *17*, 117−126.
(80) Kállay, M.; Gauss, J. Calculation of Excited-State Properties Using General Coupled-Cluster and Configuration-Interaction Models. *J. Chem. Phys.* **2004**, *121*, 9257−9269.
(81) Kállay, M.; Gauss, J. Approximate treatment of higher excitations in coupled-cluster theory. *J. Chem. Phys.* **2005**, *123*, 214105.
(82) Loos, P.-F.; Matthews, D. A.; Lipparini, F.; Jacquemin, D. How accurate are EOM-CC4 vertical excitation energies? *J. Chem. Phys.* **2021**, *154*, 221103.
(83) Loos, P.-F.; Lipparini, F.; Matthews, D. A.; Blondel, A.; Jacquemin, D. A Mountaineering Strategy to Excited States: Revising Reference Values with EOM-CC4. *J. Chem. Theory Comput.* **2022**, *18*, 4418−4427.
(84) Rowe, D. J. Equations-of-Motion Method and the Extended Shell Model. *Rev. Mod. Phys.* **1968**, *40*, 153−166.
(85) Emrich, K. An extension of the coupled cluster formalism to excited states (I). *Nucl. Phys. A* **1981**, *351*, 379−396.
(86) Sekino, H.; Bartlett, R. J. A linear response, coupled-cluster theory for excitation energy. *Int. J. Quantum Chem.* **1984**, *26*, 255−265.
(87) Geertsen, J.; Rittby, M.; Bartlett, R. J. The equation-of-motion coupled-cluster method: Excitation energies of Be and CO. *Chem. Phys. Lett.* **1989**, *164*, 57−62.
(88) Comeau, D. C.; Bartlett, R. J. The equation-of-motion coupled-cluster method. Applications to open- and closed-shell reference states. *Chem. Phys. Lett.* **1993**, *207*, 414−423.
(89) Monkhorst, H. J. Calculation of properties with the coupled-cluster method. *Int. J. Quantum Chem.* **1977**, *12*, 421−432.
(90) Dalgaard, E.; Monkhorst, H. J. Some aspects of the time-dependent coupled-cluster approach to dynamic response functions. *Phys. Rev. A* **1983**, *28*, 1217−1222.
(91) Koch, H.; Jørgensen, P. Coupled cluster response functions. *J. Chem. Phys.* **1990**, *93*, 3333−3344.
(92) Pawłowski, F.; Jørgensen, P.; Hättig, C. Gauge invariance of oscillator strengths in the approximate coupled cluster triples model CC3. *Chem. Phys. Lett.* **2004**, *389*, 413−420.
(93) Sarkar, R.; Boggio-Pasqua, M.; Loos, P.-F.; Jacquemin, D. Benchmarking TD-DFT and Wave Function Methods for Oscillator Strengths and Excited-State Dipole Moments. *J. Chem. Theory Comput.* **2021**, *17*, 1117−1132.
(94) Giner, E.; Pradines, B.; Ferté, A.; Assaraf, R.; Savin, A.; Toulouse, J. Curing Basis-Set Convergence Of Wave-Function Theory Using Density-Functional Theory: A Systematically Improvable Approach. *J. Chem. Phys.* **2018**, *149*, 194301.
(95) Traore, D.; Toulouse, J.; Giner, E. Basis-set correction for coupled-cluster estimation of dipole moments. *J. Chem. Phys.* **2022**, *156*, 174101.
(96) Pople, J. A.; Krishnan, R.; Schlegel, H. B.; Binkley, J. S. Derivative studies in hartree-fock and møller-plesset theories. *Int. J. Quantum Chem.* **1979**, *16*, 225−241.
(97) Helgaker, T.; Jørgensen, P.; Handy, N. C. A numerically stable procedure for calculating Møller-Plesset energy derivatives, derived using the theory of Lagrangians. *Theor. Chim. Acta* **1989**, *76*, 227−245.
(98) Pulay, P. Ab initio calculation of force constants and equilibrium geometries in polyatomic molecules. *Mol. Phys.* **1969**, *17*, 197−204.
(99) Handy, N. C.; Schaefer, H. F. On the evaluation of analytic energy derivatives for correlated wave functions. *J. Chem. Phys.* **1984**, *81*, 5031−5033.
(100) Diercksen, G. H. F.; Roos, B. O.; Sadlej, A. J. Legitimate calculation of first-order molecular properties in the case of limited CI functions. Dipole moments. *Chem. Phys.* **1981**, *59*, 29−39.
(101) Fitzgerald, G.; Harrison, R.; Laidig, W. D.; Bartlett, R. J. Third-order MBPT gradients. *J. Chem. Phys.* **1985**, *82*, 4379−4380.
(102) Gauss, J.; Cremer, D. Implementation of analytical energy gradients at third- and fourth-order Møller-Plesset perturbation theory. *Chem. Phys. Lett.* **1987**, *138*, 131−140.
(103) Trucks, G. W.; Watts, J. D.; Salter, E. A.; Bartlett, R. J. Analytical MBPT(4) gradients. *Chem. Phys. Lett.* **1988**, *153*, 490−495.
(104) Gauss, J.; Cremer, D. Analytical differentiation of the energy contribution due to triple excitations in fourth-order Møller-Plesset perturbation theory. *Chem. Phys. Lett.* **1988**, *153*, 303−308.
(105) Tachibana, A.; Yamashita, K.; Yamabe, T.; Fukui, K. Exact formula for the gradient of the CI potential energy hypersurface. *Chem. Phys. Lett.* **1978**, *59*, 255−260.
(106) Goddard, J. D.; Handy, N. C.; Schaefer, H. F. Gradient techniques for open-shell restricted Hartree−Fock and multiconfiguration self-consistent-field methods. *J. Chem. Phys.* **1979**, *71*, 1525−1530.
(107) Krishnan, R.; Schlegel, H. B.; Pople, J. A. Derivative studies in configuration−interaction theory. *J. Chem. Phys.* **1980**, *72*, 4654−4655.
(108) Brooks, B. R.; Laidig, W. D.; Saxe, P.; Goddard, J. D.; Yamaguchi, Y.; Schaefer, H. F. Analytic gradients from correlated wave functions via the two-particle density matrix and the unitary group approach. *J. Chem. Phys.* **1980**, *72*, 4652−4653.
(109) Osamura, Y.; Yamaguchi, Y.; Schaefer, H. F. Analytic configuration interaction (CI) gradient techniques for potential energy hypersurfaces. A method for open-shell molecular wave functions. *J. Chem. Phys.* **1981**, *75*, 2919−2922.
(110) Osamura, Y.; Yamaguchi, Y.; Schaefer, H. F. Generalization of analytic configuration interaction (CI) gradient techniques for potential energy hypersurfaces, including a solution to the coupled perturbed Hartree−Fock equations for multiconfiguration SCF molecular wave functions. *J. Chem. Phys.* **1982**, *77*, 383−390.
(111) Jørgensen, P.; Simons, J. Ab initio analytical molecular gradients and Hessians. *J. Chem. Phys.* **1983**, *79*, 334−357.
(112) Pulay, P. Second and third derivatives of variational energy expressions: Application to multiconfigurational self-consistent field wave functions. *J. Chem. Phys.* **1983**, *78*, 5043−5051.
(113) Yamaguchi, Y.; Schaefer, H. F. *Handbook of High-resolution Spectroscopy*; John Wiley & Sons, Ltd: Chichester, England, UK, 2011.
(114) Adamowicz, L.; Laidig, W. D.; Bartlett, R. J. Analytical gradients for the coupled-cluster method. *Int. J. Quantum Chem.* **1984**, *26*, 245−254.
(115) Fitzgerald, G.; Harrison, R. J.; Bartlett, R. J. Analytic energy gradients for general coupled-cluster methods and fourth-order many-body perturbation theory. *J. Chem. Phys.* **1986**, *85*, 5143−5150.
(116) Scheiner, A. C.; Scuseria, G. E.; Rice, J. E.; Lee, T. J.; Schaefer, H. F. Analytic evaluation of energy gradients for the single and double excitation coupled cluster (CCSD) wave function: Theory and application. *J. Chem. Phys.* **1987**, *87*, 5361−5373.
(117) Lee, T. J.; Rendell, A. P. Analytic gradients for coupled-cluster energies that include noniterative connected triple excitations: Application to cis- and trans-HONO. *J. Chem. Phys.* **1991**, *94*, 6229−6236.
(118) Gauss, J.; Stanton, J. F.; Bartlett, R. J. Coupled-cluster open-shell analytic gradients: Implementation of the direct product decomposition approach in energy gradient calculations. *J. Chem. Phys.* **1991**, *95*, 2623−2638.
(119) Gauss, J.; Stanton, J. F. Analytic first and second derivatives for the CCSDT- n (n = 1−3) models: a first step towards the efficient calculation of CCSDT properties. *Phys. Chem. Chem. Phys.* **2000**, *2*, 2047−2060.

https://doi.org/10.1021/acs.jctc.2c01111
J. Chem. Theory Comput. 2023, 19, 221−234

(120) Gauss, J.; Stanton, J. F. Analytic gradients for the coupled-cluster singles, doubles, and triples (CCSDT) model. *J. Chem. Phys.* **2002**, *116*, 1773−1782.
(121) Levine, D. S.; Hait, D.; Tubman, N. M.; Lehtola, S.; Whaley, K. B.; Head-Gordon, M. CASSCF with Extremely Large Active Spaces Using the Adaptive Sampling Configuration Interaction Method. *J. Chem. Theory Comput.* **2020**, *16*, 2340−2354.
(122) Park, J. W. Near-Exact CASSCF-Level Geometry Optimization with a Large Active Space using Adaptive Sampling Configuration Interaction Self-Consistent Field Corrected with Second-Order Perturbation Theory (ASCI-SCF-PT2). *J. Chem. Theory Comput.* **2021**, *17*, 4092−4104.
(123) Smith, J. E. T.; Lee, J.; Sharma, S. Near-exact nuclear gradients of complete active space self-consistent field wave functions. *J. Chem. Phys.* **2022**, *157*, 094104.
(124) Jiang, T.; Fang, W.; Alavi, A.; Chen, J. General Analytical Nuclear Forces and Molecular Potential Energy Surface from Full Configuration Interaction Quantum Monte Carlo. *J. Chem. Theory Comput.* **2022**, *18* (12), 7233.
(125) Vaval, N.; Pal, S. A fully relaxed extended coupled-cluster approach for molecular properties. *Chem. Phys. Lett.* **2004**, *398*, 194−200.
(126) Trucks, G. W.; Salter, E. A.; Sosa, C.; Bartlett, R. J. Theory and implementation of the MBPT density matrix. An application to one-electron properties. *Chem. Phys. Lett.* **1988**, *147*, 359−366.
(127) Helgaker, T.; Jørgensen, P. Configuration-interaction energy derivatives in a fully variational formulation. *Theor. Chim. Acta* **1989**, *75*, 111−127.
(128) Koch, H.; Jensen, H. J. Aa.; Jørgensen, P.; Helgaker, T.; Scuseria, G. E.; Schaefer, H. F. Coupled cluster energy derivatives. Analytic Hessian for the closed-shell coupled cluster singles and doubles wave function: Theory and applications. *J. Chem. Phys.* **1990**, *92*, 4924−4940.
(129) Jørgensen, P.; Helgaker, T. Mo/ller−Plesset energy derivatives. *J. Chem. Phys.* **1988**, *89*, 1560−1570.
(130) Hodecker, M.; Rehn, D. R.; Dreuw, A.; Höfener, S. Similarities and differences of the Lagrange formalism and the intermediate state representation in the treatment of molecular properties. *J. Chem. Phys.* **2019**, *150*, 164125.
(131) Koch, H.; Kobayashi, R.; Sanchez de Merás, A.; Jorgensen, P. Calculation of size-intensive transition moments from the coupled cluster singles and doubles linear response function. *J. Chem. Phys.* **1994**, *100*, 4393−4400.
(132) Baeck, K. K.; Watts, J. D.; Bartlett, R. J. Analytic energy gradients with frozen molecular orbitals in coupled-cluster and many-body perturbation theory methods: Systematic study of the magnitude and trends of the effects of frozen molecular orbitals. *J. Chem. Phys.* **1997**, *107*, 3853−3863.
(133) List, N. H.; Melin, T. R. L.; van Horn, M.; Saue, T. Beyond the electric-dipole approximation in simulations of x-ray absorption spectroscopy: Lessons from relativistic theory. *J. Chem. Phys.* **2020**, *152*, 184110.
(134) Pedersen, T. B.; Koch, H. Coupled cluster response functions revisited. *J. Chem. Phys.* **1997**, *106*, 8059−8072.
(135) Sauer, S. P. A.; Sabin, J. R.; Oddershede, J. Calculation of mean excitation energies. *Adv. Quantum Chem.* **2019**, *80*, 225−245.
(136) Thomas, W. Über die Zahl der Dispersionselektronen, die einem stationären Zustande zugeordnet sind. *Naturwissenschaften* **1925**, *13*, 627.
(137) Reiche, F.; Thomas, W. Über die Zahl der Dispersionselektronen, die einem stationären Zustand zugeordnet sind. *Z. Phys.* **1925**, *34*, 510.
(138) Kuhn, W. Über die Gesamtstärke der von einem Zustande ausgehenden Absorptionslinien. *Z. Phys.* **1925**, *33*, 408.
(139) Pedersen, T. B.; Koch, H. Gauge invariance of the coupled cluster oscillator strength. *Chem. Phys. Lett.* **1998**, *293*, 251−260.
(140) Chrayteh, A.; Blondel, A.; Loos, P.-F.; Jacquemin, D. Mountaineering Strategy to Excited States: Highly Accurate Oscillator Strengths and Dipole Moments of Small Molecules. *J. Chem. Theory Comput.* **2021**, *17*, 416.
(141) Giner, E.; Scemama, A.; Toulouse, J.; Loos, P. F. Chemically accurate excitation energies with small basis sets. *J. Chem. Phys.* **2019**, *151*, 144118.
(142) Loos, P. F.; Pradines, B.; Scemama, A.; Toulouse, J.; Giner, E. A Density-Based Basis-Set Correction for Wave Function Theory. *J. Phys. Chem. Lett.* **2019**, *10*, 2931−2937.
(143) Giner, E.; Scemama, A.; Loos, P.-F.; Toulouse, J. A basis-set error correction based on density-functional theory for strongly correlated molecular systems. *J. Chem. Phys.* **2020**, *152*, 174104.
(144) Eriksen, J. J.; Gauss, J. Ground and excited state first-order properties in many-body expanded full configuration interaction theory. *J. Chem. Phys.* **2020**, *153*, 154107.
(145) Eriksen, J. J.; Lipparini, F.; Gauss, J. Virtual Orbital Many-Body Expansions: A Possible Route towards the Full Configuration Interaction Limit. *J. Phys. Chem. Lett.* **2017**, *8*, 4633−4639.
(146) Eriksen, J. J.; Gauss, J. Many-Body Expanded Full Configuration Interaction. I. Weakly Correlated Regime. *J. Chem. Theory Comput.* **2018**, *14*, 5180.
(147) Eriksen, J. J.; Gauss, J. Many-Body Expanded Full Configuration Interaction. II. Strongly Correlated Regime. *J. Chem. Theory Comput.* **2019**, *15*, 4873.
(148) Eriksen, J. J.; Gauss, J. Generalized Many-Body Expanded Full Configuration Interaction Theory. *J. Phys. Chem. Lett.* **2019**, *10* (24), 7910−7915.
(149) Coe, J. P.; Taylor, D. J.; Paterson, M. J. Monte Carlo configuration interaction applied to multipole moments, ionization energies, and electron affinities. *J. Comput. Chem.* **2013**, *34*, 1083−1093.
(150) Thomas, R. E.; Opalka, D.; Overy, C.; Knowles, P. J.; Alavi, A.; Booth, G. H. Analytic nuclear forces and molecular properties from full configuration interaction quantum Monte Carlo. *J. Chem. Phys.* **2015**, *143*, 054108.
(151) Hait, D.; Head-Gordon, M. How accurate are static polarizability predictions from density functional theory? An assessment over 132 species at equilibrium geometry. *Phys. Chem. Chem. Phys.* **2018**, *20*, 19800−19810.
(152) Furche, F.; Ahlrichs, R. Adiabatic Time-Dependent Density Functional Methods for Excited State Properties. *J. Chem. Phys.* **2002**, *117*, 7433.
(153) Tawada, Y.; Tsuneda, T.; Yanagisawa, S.; Yanai, T.; Hirao, K. A Long-Range-Corrected Time-Dependent Density Functional Theory. *J. Chem. Phys.* **2004**, *120*, 8425−8433.
(154) Miura, M.; Aoki, Y.; Champagne, B. Assessment of Time-Dependent Density Functional Schemes for Computing The Oscillator Strengths of Benzene, Phenol, Aniline, and Fluorobenzene. *J. Chem. Phys.* **2007**, *127*, 084103.
(155) Timerghazin, Q. K.; Carlson, H. J.; Liang, C.; Campbell, R. E.; Brown, A. Computational Prediction of Absorbance Maxima for a Structurally Diverse Series of Engineered Green Fluorescent Protein Chromophores. *J. Phys. Chem. B* **2008**, *112*, 2533−2541.
(156) Silva-Junior, M. R.; Schreiber, M.; Sauer, S. P. A.; Thiel, W. Benchmarks for Electronically Excited States: Time-Dependent Density Functional Theory and Density Functional Theory Based Multireference Configuration Interaction. *J. Chem. Phys.* **2008**, *129*, 104103.
(157) King, R. A. On the Accuracy of Computed Excited-State Dipole Moments. *J. Phys. Chem. A* **2008**, *112*, 5727−5733.
(158) Wong, B. M.; Piacenza, M.; Della Sala, F. Absorption and Fluorescence Properties of Oligothiophene Biomarkers from Long-Range-Corrected Absorption and Fluorescence Properties of Oligothiophene Biomarkersfrom Long-Range-Corrected Time-Dependent Density Functional Theory. *Phys. Chem. Chem. Phys.* **2009**, *11*, 4498−4508.
(159) Tapavicza, E.; Tavernelli, I.; Rothlisberger, U. Ab Initio Excited State Properties and Dynamics of a Prototype σ-Bridged-Donor-Acceptor Molecule. *J. Phys. Chem. A* **2009**, *113*, 9595−9602.

https://doi.org/10.1021/acs.jctc.2c01111
J. Chem. Theory Comput. 2023, 19, 221−234

(160) Guido, C. A.; Jacquemin, D.; Adamo, C.; Mennucci, B. On the TD-DFT Accuracy in Determining Single and Double Bonds in Excited-State Structures of Organic Molecules. *J. Phys. Chem. A* **2010**, *114*, 13402−13410.
(161) Silva-Junior, M. R.; Thiel, W. Benchmark of Electronically Excited States for Semiempirical Methods: MNDO, AM1, PM3, OM1, OM2, OM3, INDO/S, and INDO/S2. *J. Chem. Theory Comput.* **2010**, *6*, 1546−1564.
(162) Caricato, M.; Trucks, G.; Frisch, M.; Wiberg, K. Oscillator Strength: How Does TDDFT Compare to EOM-CCSD? *J. Chem. Theory Comput.* **2011**, *7*, 456−466.
(163) Hellweg, A. The Accuracy of Dipole Moments from Spin-Component Scaled CC2 in Ground and Electronically Excited States. *J. Chem. Phys.* **2011**, *134*, 064103.
(164) Szalay, P. G.; Watson, T.; Perera, A.; Lotrich, V. F.; Bartlett, R. J. Benchmark Studies on the Building Blocks of DNA. 1. Superiority of Coupled Cluster Methods in Describing the Excited States of Nucleobases in the Franck−Condon Region. *J. Phys. Chem. A* **2012**, *116*, 6702−6710.
(165) Kánnár, D.; Szalay, P. G. Benchmarking Coupled Cluster Methods on Valence Singlet Excited States. *J. Chem. Theory Comput.* **2014**, *10*, 3757−3765.
(166) Sauer, S. P.; Pitzner-Frydendahl, H. F.; Buse, M.; Jensen, H. J. A.; Thiel, W. Performance of SOPPA-Based Methods in the Calculation of Vertical Excitation Energies and Oscillator Strengths. *Mol. Phys.* **2015**, *113*, 2026−2045.
(167) Jacquemin, D.; Duchemin, I.; Blondel, A.; Blase, X. Assessment of the Accuracy of the Bethe-Salpeter (BSE/GW) Oscillator Strengths. *J. Chem. Theory Comput.* **2016**, *12*, 3969−3981.
(168) Jacquemin, D. Excited-State Dipole and Quadrupole Moments: TD-DFT versus CC2. *J. Chem. Theory Comput.* **2016**, *12*, 3993−4003.
(169) Robinson, D. Comparison of the Transition Dipole Moments Calculated by TDDFT with High Level Wave Function Theory. *J. Chem. Theory Comput.* **2018**, *14*, 5303−5309.
(170) Hodecker, M.; Dreuw, A. Unitary Coupled Cluster Ground- and Excited-State Molecular Properties. *J. Chem. Phys.* **2020**, *153*, 084112.
(171) Scemama, A.; Caffarel, M.; Benali, A.; Jacquemin, D.; Loos, P. F. Influence of Pseudopotentials on Excitation Energies from Selected Configuration Interaction and Diffusion Monte Carlo. *Res. Chem.* **2019**, *1*, 100002.
(172) Scemama, A.; Giner, E. An efficient implementation of Slater-Condon rules. *arXiv* **2013**, 1311.6244.
(173) Kállay, M.; et al. The MRCC program system: Accurate quantum chemistry from water to proteins. *J. Chem. Phys.* **2020**, *152*, 074107.
(174) Loos, P. F.; Scemama, A.; Blondel, A.; Garniron, Y.; Caffarel, M.; Jacquemin, D. A Mountaineering Strategy to Excited States: Highly-Accurate Reference Energies and Benchmarks. *J. Chem. Theory Comput.* **2018**, *14*, 4360.
(175) Loos, P.-F.; Boggio-Pasqua, M.; Scemama, A.; Caffarel, M.; Jacquemin, D. Reference Energies for Double Excitations. *J. Chem. Theory Comput.* **2019**, *15*, 1939−1956.
(176) Loos, P.-F.; Scemama, A.; Jacquemin, D. The Quest for Highly Accurate Excitation Energies: A Computational Perspective. *J. Phys. Chem. Lett.* **2020**, *11*, 2374−2383.
(177) Loos, P. F.; Lipparini, F.; Boggio-Pasqua, M.; Scemama, A.; Jacquemin, D. A Mountaineering Strategy to Excited States: Highly-Accurate Energies and Benchmarks for Medium Sized Molecules. *J. Chem. Theory Comput.* **2020**, *16*, 1711−1741.
(178) Loos, P.-F.; Scemama, A.; Boggio-Pasqua, M.; Jacquemin, D. Mountaineering Strategy to Excited States: Highly Accurate Energies and Benchmarks for Exotic Molecules and Radicals. *J. Chem. Theory Comput.* **2020**, *16*, 3720−3736.
(179) Véril, M.; Scemama, A.; Caffarel, M.; Lipparini, F.; Boggio-Pasqua, M.; Jacquemin, D.; Loos, P.-F. QUESTDB: A database of highly accurate excitation energies for the electronic structure community. *WIREs Comput. Mol. Sci.* **2021**, *11*, e1517.
(180) Chilkuri, V. G.; Applencourt, T.; Gasperich, K.; Loos, P.-F.; Scemama, A. Spin-Adapted Selected Configuration Interaction in a Determinant Basis. *Adv. Quantum Chem.* **2021**, *83*, 65.
(181) Angeli, C.; Cimiraglia, R.; Evangelisti, S.; Leininger, T.; Malrieu, J.-P. Introduction of *n* -Electron Valence States for Multireference Perturbation Theory. *J. Chem. Phys.* **2001**, *114*, 10252−10264.

https://doi.org/10.1021/acs.jctc.2c01111
J. Chem. Theory Comput. 2023, 19, 221−234